2018

Fast And Accurate Co2 Properties Calculation Algorithm For Massive Numerical Simulations Of Supersonic Two-phase Ejectors

Yu Fang
"Université Catholique de Louvain, Belgium; Université de Sherbrooke, Canada", yu.fang@uclouvain.be

Marco De Lorenzo
IMSIA UMR EDF-CNRS-CEA-ENSTA, France, marco.de-lorenzo@edf.fr

Philippe Lafon
IMSIA UMR EDF-CNRS-CEA-ENSTA, France, philippe.lafon@edf.fr

Sébastien Poncet
Université de Sherbrooke, Canada, sebastien.poncet@usherbrooke.ca

Yann Bartosiewicz
Université Catholique de Louvain, Belgium, yann.bartosiewicz@uclouvain.be

See next page for additional authors

Fast And Accurate CO2 Properties Calculation Algorithm For Massive Numerical Simulations Of Supersonic Two-phase Ejectors

Yu Fang[1,3, *], Marco De Lorenzo[2], Philippe Lafon[2], Sébastien Poncet[3], Yann Bartosiewicz[1], Hakim Nesreddine[4]

[1] Université catholique de Louvain, Institute of Mechanics, Materials, and Civil Engineering (iMMC)
1348 Louvain-la-Neuve, Belgium
Phone: +32 10 47 22 06, E-mail: yann.bartosiewicz@uclouvain.be

[2] IMSIA UMR EDF-CNRS-CEA-ENSTA,
Paris, France
Phone: +33 1 78 19 38 27, E-mail: philippe.lafon@edf.fr

[3] Université de Sherbrooke, Sherbrooke, Québec, Canada
Phone: +1 819 821-8000, E-mail: Sebastien.Poncet@USherbrooke.ca

[4] Laboratoire des technologies de l'énergie, Shawinigan, Québec, Canada
Phone: +1 819 539-1400, E-mail: Nesreddine.Hakim@ireq.ca

[*]Corresponding Author: Yu.Fang@USherbrooke.ca

ABSTRACT

This work presents a look-up table method to compute the thermodynamic properties of CO2. It is motivated by the massive employment of this fluid in the industrial domain, especially in the ejector-expansion cycle. Computational Fluid Dynamics simulations have been used in the past to investigate two-phase ejector flows. CO2 exhibits large property variations due to phase transition. As a result, it cannot be accurately modelled by a general analytical Equation of State (EoS), such as Peng-Robinson EoS, or Perfect gas EoS, etc. Hence, a tabulated EoS is developed here based on the Span-Wagner (EoS), covering the temperature range from 217 K to 800 K and pressures up to 50 MPa. Supercritical, liquid, vapor and liquid-vapor states are all included in this tabulated EoS. Besides, the density and the internal energy are chosen as two independent inputs to compute the other properties. The method is designed to be coupled with the system of equations in its conservative form which is a usual formulation for compressible solvers suited for ejectors. Through two validation cases, the proposed tabulated EoS shows good performances in terms of accuracy and efficiency, making it suitable for future massive CFD simulations.

1. INTRODUCTION

The application of the two-phase CO_2 ejector in the refrigeration system has been significantly investigated since the last decade. Replacing the expansion valve by a two-phase ejector results indeed in reduced throttling losses inherently associated to expansion of CO_2. The compression effect produced by the ejector can also reduce the compressor load. As a result, the cooling capacity increases and the Coefficient of Performance (COP) of the whole system is improved. The experimental investigations by Elbel and Hrnjak (2006) and Elbel and Hrnjak (2008) showed an improvement of the COP and cooling capacity by 7% and 8%, respectively. Li and Groll (2004) and Li and Groll (2005) provided simulation results of a CO_2 transcritical air-conditioning system with an ejector. They reported a COP improvement up to 16%. Besides, in the context of refrigeration, considering CO_2 as the working fluid has several advantages: low costs, non-toxic, low Global Warming Potential (GWP) and zero Ozone Depletion Potential (ODP). It appears then

as a promising alternative to synthetic refrigerants in future energy conversion systems and in the refrigeration industry.

A standard system using a CO_2 two-phase ejector for expansion work recovery is shown in Fig. 1. The supercritical CO_2 fluid exiting the gas cooler is expanded in the motive nozzle of the ejector. The motive fluid gains considerable kinetic energy, while decreasing the pressure. As a result, the CO_2 fluid is under a supercritical state on the liquid side (point 3), then crosses the liquid saturation curve and finally becomes liquid-vapor state (point 4). This rapid phase transition is usually named 'flashing'. It occurs often near the nozzle throat. Due to the phase transition, the speed of sound decreases rapidly, thus the flow can become supersonic immediately. At the exit of the motive nozzle, a low-pressure supersonic two-phase jet flows into the secondary nozzle. Then, it can entrain the secondary vapor flow from the evaporator. These two flows exchange momentum and heat (exergy) by the turbulent mixing. Shock waves may occur during this mixing process and the separation of the boundary layer can be encountered as well, as a results of shock-boundary layer interactions. Finally, the mixed stream compresses in the diffuser (by pressure recovery due to kinetic energy conversion) before entering the liquid-vapor separator. Complicated physical phenomena can happen then in the two-phase ejector; therefore, it is important to understand them for predicting the real flow physics along this device.

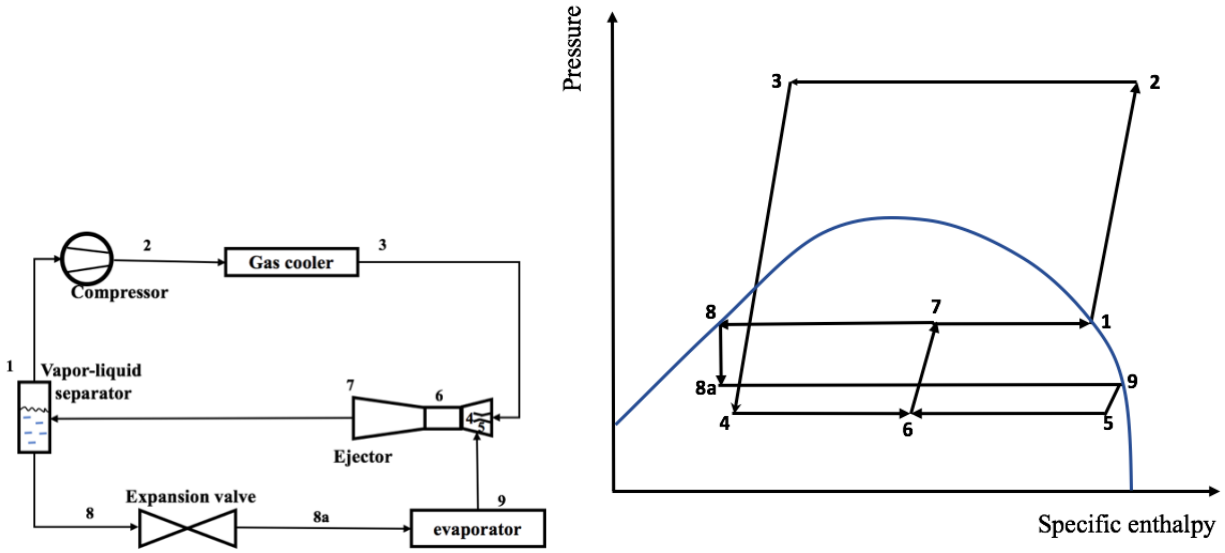

Figure 1: Schematic of a transcritical CO_2 refrigeration cycle using a two-phase ejector for expansion work recovery and the corresponding p-h diagram.

Computational Fluid Dynamic (CFD) simulations have been extensively used recently to predict the flow behavior in two-phase ejectors. However, Raman and Kim (2018) proved that the Equation of State (EoS) which computes the thermodynamic properties of CO_2 during the simulations has a strong influence on the results. Hence, it is mandatory to calculate the accurate properties of CO_2 whatever it is liquid, vapor or liquid-vapor. In the literature, Refprop (Lemmon et al., 2010) is the most used library for CO_2 properties, which is based on the Span-Wagner (SW) EoS. It was used by Yazdani et al. (2012), Colarossi et al. (2012) and Smolka et al. (2013). It provided fairly good numerical results for two-phase ejectors, but the computational time was also prohibitively high by using direct coupling. The present objective in a near future is to conduct massive CFD simulations (*i.e.* 3D unsteady Large-Eddy Simulations) for which millions of mesh points are required. It is then necessary to compute the CO_2 properties accurately and efficiently.

The look-up table method is a good candidate to satisfy these two requirements. It has been well-known and already used for water-steam fast transient simulations in nuclear thermodynamics (Kunick et al., 2008; De Lorenzo et al., 2017) and cavitating flows (Khatami et al., 2015). This property calculation process is quasi-instantaneous and provides highly accurate results. Similarly, a Refprop based table within CFX was proposed by Ameli et al. (2017) for the simulation of a CO_2 nozzle. The liquid, vapor, vapor metastable and saturated states were included in the table.

However, due to the limitation of the commercial software, this table does not give the flexibility of a full in-house approach to optimize the accuracy and the efficiency, as well as using various two-phase models (Homogeneous Relaxation Model, Delayed Equilibrium Model) (Bilicki and Kestin,1990; Bartosiewicz and Seynhaeve,2013). Hence, in this work, an in-house tabulated EoS was developed by extending the work of De Lorenzo et al. (2017) and it is suitable for most of the compressible solver working with conservative variables.

2. LOOK-UP TABLE METHOD

As mentioned above, this tabulated method is suited for any system of equations in their conservative form. It means that the properties, such as the pressure, temperature, and speed of sound are computed by using the density and the internal energy (ρ, e), which are obtained directly from the system of equations. Therefore, the tabulation is done in the ρ-e space (or v-e space, where v is the specific volume).

2.1 Property calculation procedure

Firstly, a mesh is built in the v-e space prior to the CFD simulation and at each node (v, e), the properties are computed based on the original Span-Wagner EoS. The values are stored as variables in the memory. The v-e space is depicted in Fig. 2. The maximum pressure is fixed to 50 MPa as the left limit and the minimum pressure is fixed to 0.5 MPa as the right limit for the table. The Perfect-gas EoS is applied to complete the small pressure region, where pressures are smaller than 0.5 MPa. The maximum internal energy is 540 $kJ.kg^{-1}$ corresponding to approximately 800 K. The bottom limit is the internal energy of liquid at the triple point (approximately 217 K). The saturation curve is shown in the v-e space, as shown in Fig. 2.

The region wrapped by the saturation curve and the isobaric curve of the triple point is the liquid-vapor region. Here, the Homogeneous Equilibrium Model is considered, which means that the liquid phase and the vapor phase are always in thermodynamic and mechanical equilibrium.

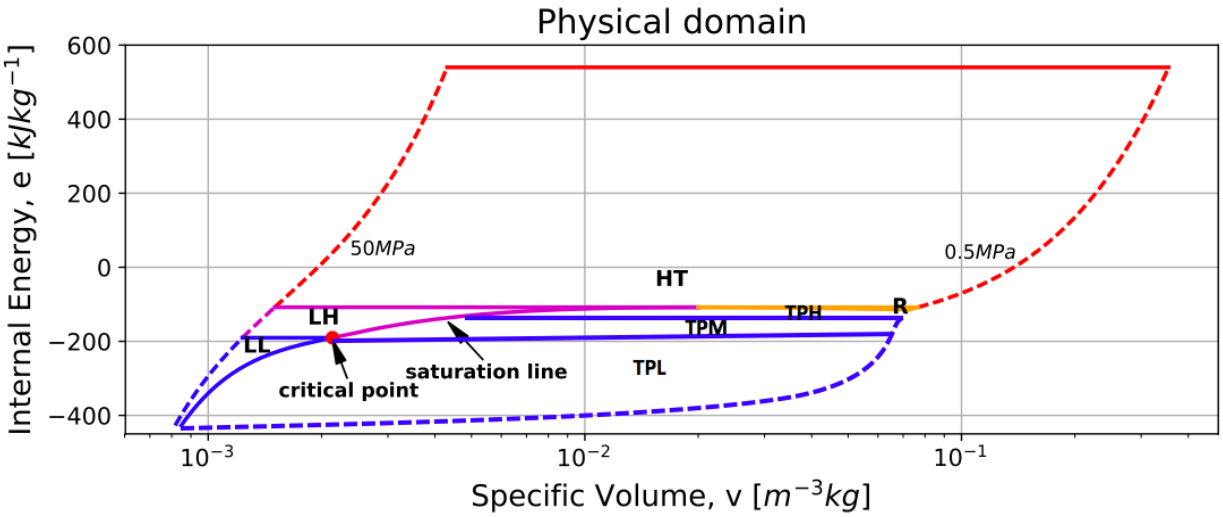

Figure 2: e-v space with pressure from 0.5MPa to 50MPa and temperature from 216.5K to approximate 800K. The computed region is divided into several sub-regions, denoted LL, LH, HT, R for the single-phase regions and TPL, TPM, TPH for the liquid-vapor phases.

During the CFD simulation, a pair of (v, e) is firstly found in one cell of one sub-region and then the properties are computed by using the bilinear interpolation in a regular X-Y space as it can improve the accuracy of the interpolation. An example is illustrated in Fig. 3. Firstly, the cell in the v-e space which the pair (v_0, e_0) belongs to is found and simultaneously the corresponding (X_0, Y_0) in the X-Y space is determined.

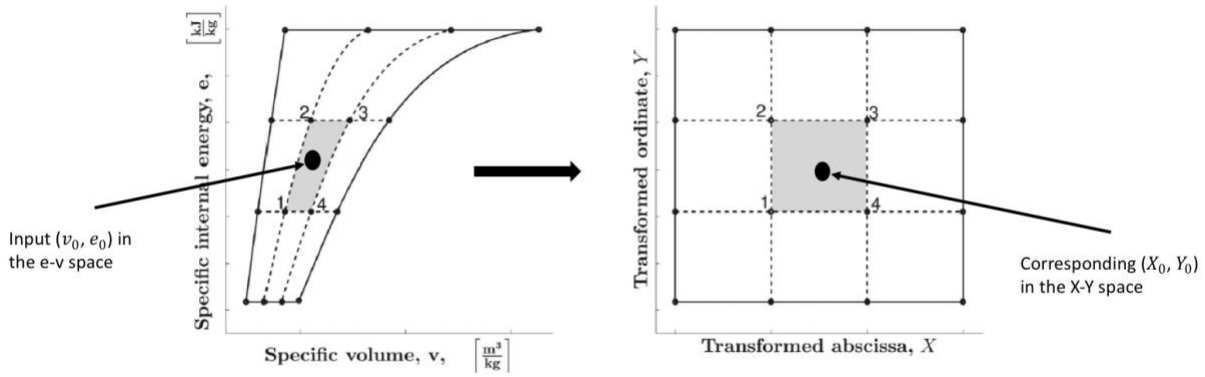

Figure 3: Mapped v-e space and X-Y space from De Lorenzo et al. (2017). The numbering of vertices for one cell starts from the left bottom corner and is counted in the clockwise direction.

Then, the properties are computed by the values at the four vertices of the cell. For example, the pressure can be expressed as:

$$p\,(e_0, v_0) = \tilde{p}\,(X_0, Y_0) = \gamma_1 + \gamma_2 X_0 + \gamma_3 Y_0 + \gamma_4 X_0 Y_0, \tag{1}$$

where γ1, γ2, γ3 and γ4 are interpolation coefficients which are obtained by the pressure values at the four vertices. One can refer to the paper (De Lorenzo et al., 2017) for the explicit formulation of the coefficients. The temperature and the speed of sound can be computed in the same manner. All the interpolation coefficients are computed in the mesh-construction stage and also stored in the memory.

2.2 Span-Wagner equation of state

The Span-Wagner EoS (Span and Wagner, 1994) is considered as the reference EoS for CO_2. It is based on hundreds of parameters that are fitted by extensive experimental data in terms of pressure, heat capacity, speed of sound, etc. The Span-Wagner EoS covers a wide range of temperature and pressure, from the triple point to 1100 K and pressures up to 800 MPa. The formulation stems from the specific Helmholtz free energy *A*, in dimensionless form $\varphi = A/RT$, respect to the reduced temperature, $\tau = T_c / T$ and the reduced density, $\delta = \rho / \rho_c$, ρ_c and T_c are the critical density and temperature, respectively. The formulation reads:

$$\varphi\,(\delta, \tau) = \varphi^0(\delta, \tau) + \varphi^r\,(\delta, \tau), \tag{2}$$

where φ consists of two parts, the ideal part φ^0 and the residual part φ^r. This residual part ensures the non-linear behavior of EoS near the critical point. Therefore, the Span-Wagner EoS can provide accurate properties in the critical region. The thermodynamic properties can be derived from the combination of the first and second derivatives of the Helmholtz energy, such as the pressure and the speed of sound (the enthalpy, entropy, and heat capacity can also be found (Span and Wagner, 1994)):

$$p\,(\delta, \tau) = \rho RT\,(1 + \delta\varphi^r_\delta), \tag{3}$$

$$c^2\,(\delta, \tau) = RT\,(1 + 2\delta\varphi^r_\delta + \delta^2\varphi^r_{\delta\delta} - \frac{(1+\delta\varphi^r_\delta - \delta\tau\varphi^r_{\delta\tau})}{\tau^2(\varphi^0_{\tau\tau} + \varphi^r_{\tau\tau})}), \tag{4}$$

where the subscript δ and τ represent the derivatives respectively to δ and τ. It can be seen that the EoS depends on the density and the temperature instead of the density and the internal energy. If one expects to use the Span-Wagner EoS directly in a simulation, an iterative algorithm is needed to inverse the EoS to compute the correct temperature corresponding to the given (v, e). Afterwards with the correct (v, T), all properties can be obtained by the Span-Wagner

EoS. The Newton-Raphson algorithm is often used for the inversion of the EoS, but the stability usually depends on the initial guess. Moreover, this iterative algorithm requires a large computational time and it should be used at each node of the mesh and at each time step. Hence, it should be avoided during CFD simulations. Although for the tabulated EoS the iterative algorithm is also used one time before the simulation for the mesh construction, the time compared to the whole CFD simulation is neglected.

2.3 Validation of the tabulated EoS

The tabulated EoS is validated by comparing the interpolated values from the tabulated EoS and the values from the original Span-Wagner EoS. The relative error of pressure and the temperature absolute error are evaluated. The error maps are displayed in Fig. 4 and 5 for the pressure and temperature, respectively. There are 25 test points in each cell in the single-phase region and 250000 test-points in the two-phase region are computed to verify that the interpolation values in any cell are accurate. Consequently, it represents a total of 2 million test points through the whole domain. It can be seen on Fig. 4 that the relative error in terms of pressure remains under 0.5%. At the same time, the absolute error in terms of temperature remains under 0.08 K as shown on Fig. 5. In fact, the large errors can be found in the neighborhood of the critical point where there are more non-linear variations. However, regarding the computational time taken by the bilinear interpolation and the accuracy that it reaches, this tabulated EoS is suitable for future massive CFD simulations.

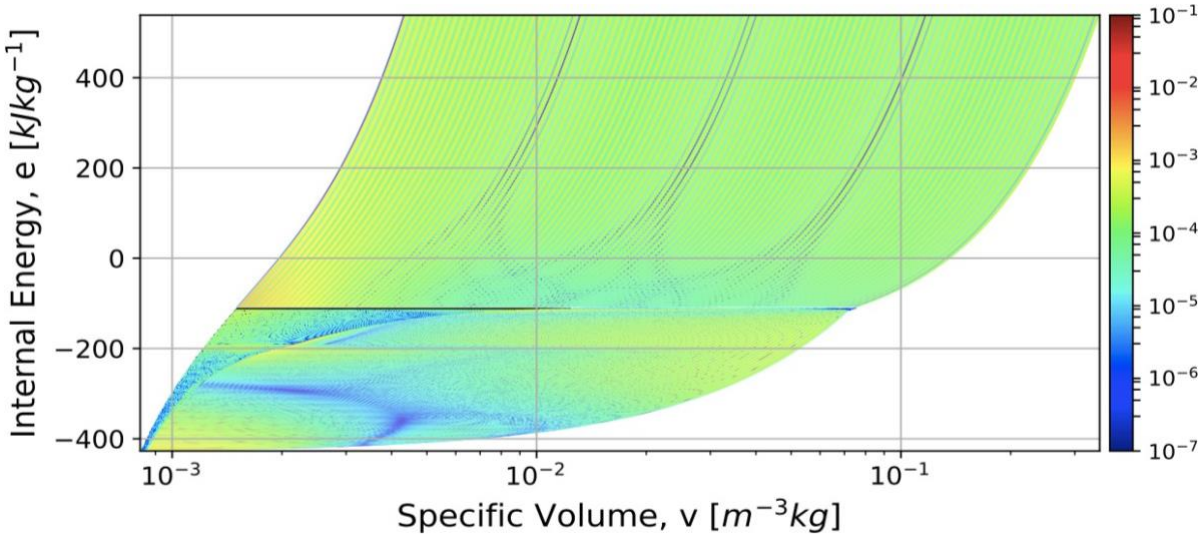

Figure 4: Relative error for the pressure in the e-v space.

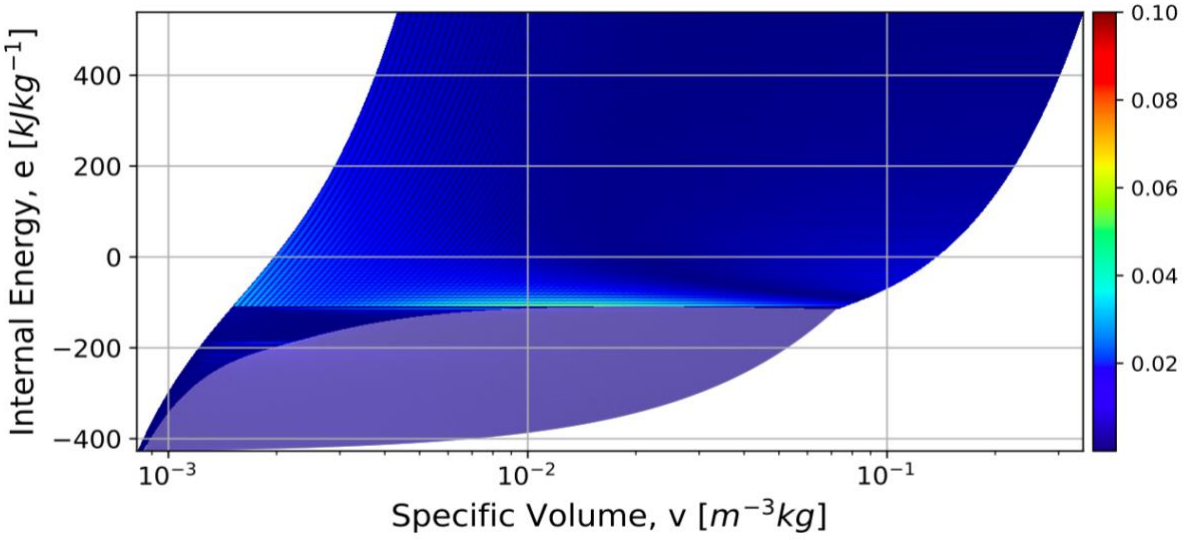

Figure 5: Absolute error for the temperature in the e − v space.

3. NUMERICAL RESULS

The proposed tabulated approach is coupled with CLAWPACK solver (LeVeque and Berger, 2017; LeVeque, 1997) which solves the Euler equations in their conservative form. The wave propagation method (Godunov, 1959) is used and an HLLC-type Riemann solver (Toro, 1997; Toro et al., 1994) is implemented in order to construct the flux at the boundary of the control volume. 1D and 2D validation cases are presented in the following.

3.1 Comparisons with different EoS

A classic shock tube problem is simulated, and the chosen conditions make sure that the flow states stay in the vapor region (single phase). A tube is divided by a membrane in the middle. The left part is filled with high pressure CO_2, ρ_L = 85.31 $kg.m^{-3}$, T_L = 360 K, and u_L = 0 $m.s^{-1}$. The initial conditions at the right side are fixed to: ρ_R = 15.1 kg.m^{-3}, T_R = 360 K and u_R = 0 m.s^{-1}. The subscripts L, R represent the left and right states, respectively. Initially, the membrane is removed, and the two fluids are in contact in the middle of the tube. A shock wave forms and propagates to the right, while an expansion wave propagates to the left. Different EoS are evaluated such as the Stiffened-Gas EoS, the Peng-Robinson EoS, the original Span-Wagner EoS and the tabulated EoS.

Table 1: Computational time and speed-up factor for different EoS.

Simulation time =1.5ms	**CPU time**	**Speed-up t_{ref} / t**
Tabulated EoS	1.67	66.16
Peng-Robinson EoS	3.35	32.98
Stiffened gas EoS	0.85	129.9
Span-Wagner EoS	110.49	1.0

The profiles of pressure, density, axial velocity and speed of sound are reported in Fig. 6. The original Span-Wagner EoS and the tabulated EoS match perfectly for all quantities. The computational time and the speed-up factor are summarized in Tab. 1. Here, the CPU time using the original Span-Wagner EoS is considered as the reference time. The speed-up factor is defined as t_{ref}/t. The tabulated EoS shows a significant speed-up compared to the reference while producing very similar results as shown previously.

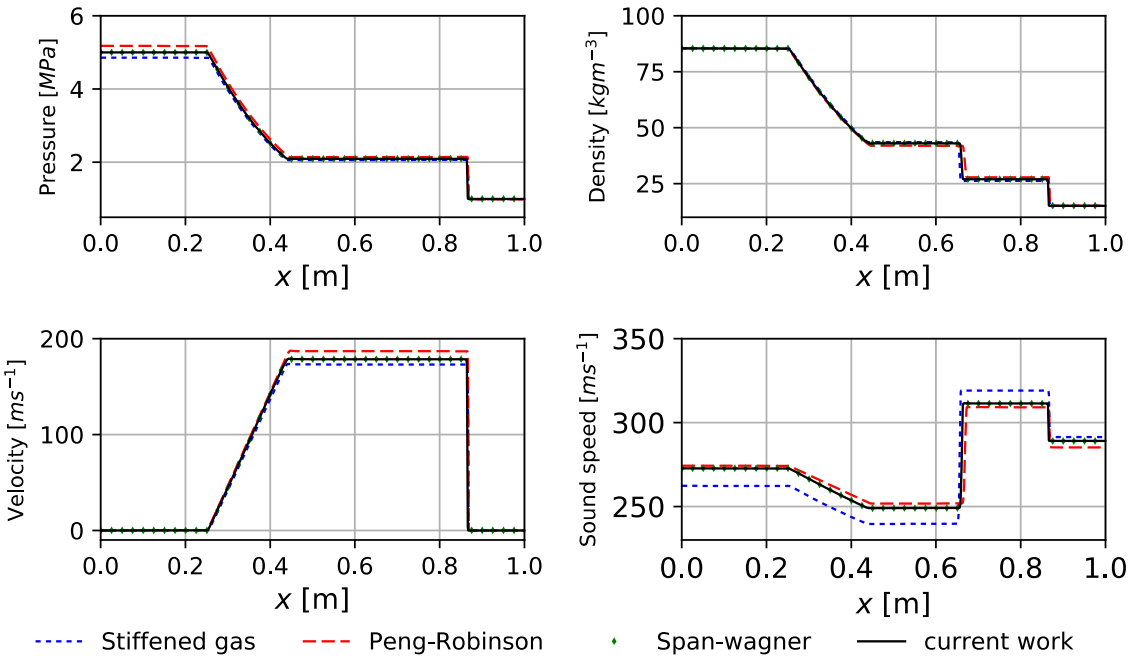

Figure 6: Streamwise distribution of pressure, density, axial velocity and speed of sound along the tube using different EoS.

Even though the Stiffened-Gas EoS is the fastest one, it may encounter some difficulties when a large variation of phase states happens in the simulation. The phase states computed by Stiffened-Gas EoS are indeed validated around a reference state which is defined by the user. For different simulations, the reference state is different depending on the range of phase states. For two-phase CO_2 simulations, it may be not suitable due to the difficulty to calibrate the reference state during the simulation, especially when the liquid, vapor and liquid-vapor states coexist.

3.2 Two-phase converging-diverging nozzle

The converging-diverging nozzle is an important part in a two-phase CO_2 ejector, converting pressure energy into kinetic energy, which allows to entrain the secondary flow. Moreover, the interesting 'flashing' phenomenon occurs in the converging-diverging nozzle, which has not been fully understood yet. Here, a 2D converging-diverging nozzle is investigated with similar operating conditions as in two-phase CO_2 ejector applications. The inlet conditions are p = 9.1 MPa and T = 309.65 K, while at the outlet, the pressure is fixed to 0.5 MPa. CO_2 is in the supercritical state at the inlet and in the two-phase state at the outlet. The flow reaches sonic conditions near the throat and accelerates until Mach = 2 at the outlet without any shock in the nozzle. The simulated nozzle was investigated experimentally by Nakagawa et al. (2009). The total length of the nozzle is 83.50 mm and the diverging angle is 0.612° as presented in Fig. 7.

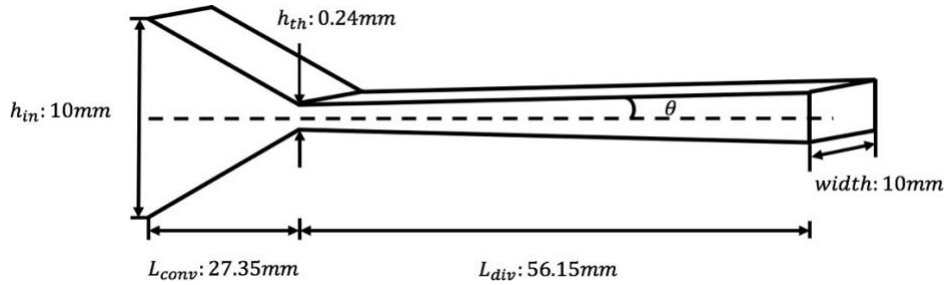

Figure 7: Schematic view of the converging-diverging nozzle with its geometrical characteristics (θ = 0.612°).

The center-line profile of pressure is reported on Fig. 8 and is compared to the direct pressure measurements (red diamonds) and the saturated pressure computed from the temperature measurements both by Nakagawa et al. (2009). A small different can be found beyond the throat. It may come from the physical modelling. The two-phase model (here HEM) assumes that the two phases are in thermodynamic and mechanical equilibrium without body forces and viscous effects. Thus, the current results do not consider the viscous dissipation and the thermodynamic non-equilibrium (which may be significant around the throat).

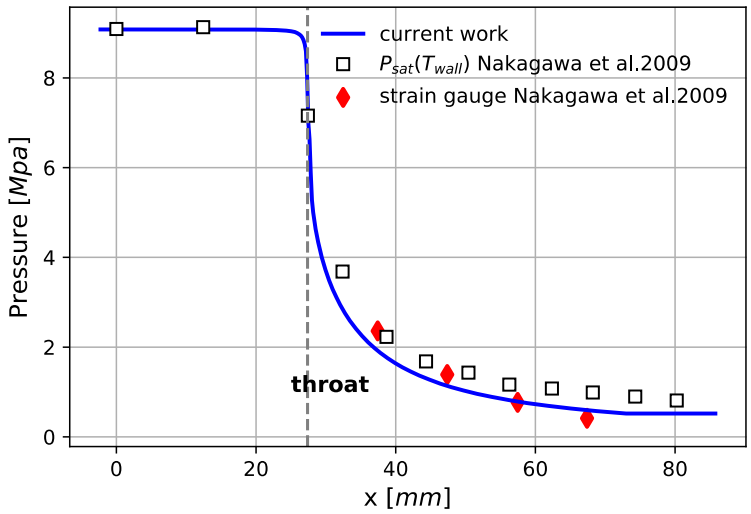

Figure 8: Pressure profile along the center line of the nozzle compared with the pressure measurements by Nakagawa et al. (2009).

As well-known, the non-equilibrium effects might have a preponderant effect within the nozzle, but there is still no convincing two-phase none-equilibrium multidimensional model able to operate under any operating conditions (Angielczyk et al., 2010; Palacz et al., 2016).

The center-line profiles of the Mach number and vapor quality in the diverging part are shown in Fig. 9. The flow becomes supersonic right at the nozzle throat meanwhile a phase transition occurs. Afterwards, the supersonic flow continues to accelerate in the diverging part and it reaches a Mach number equal to 2.4 at the outlet. There is a significant increase of vapor near the throat and through the diverging part, the vapor quality remains approximately constant around 0.5. Finally, a supersonic liquid-vapor jet rushes out of the nozzle.

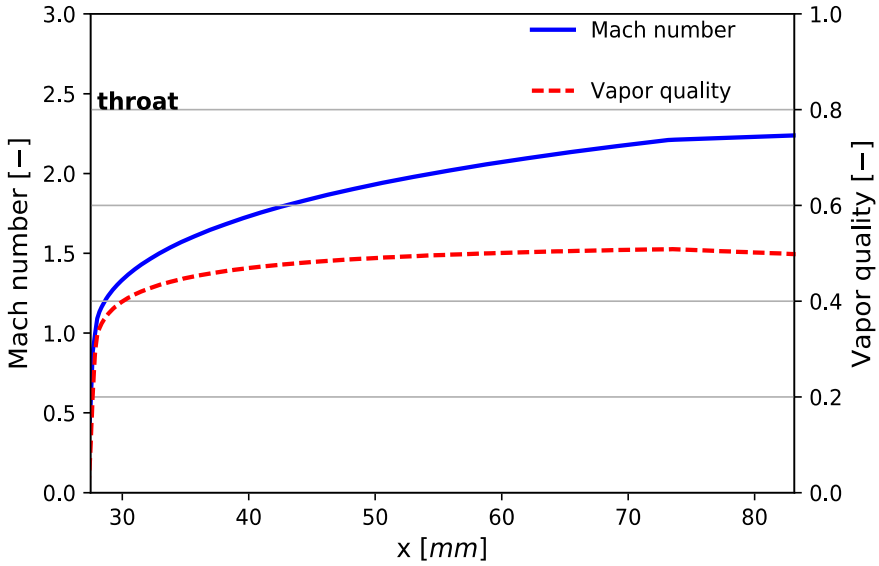

Figure 9: Vapor quality and Mach number distributions along the center line of the diverging part.

4.CONCLUSIONS

An accurate and efficient equation of state for CO_2 fluid simulations is presented in this paper. It consists in a look-up table method based on the Span-Wagner EoS, which overlays all fluid states including the supercritical, liquid, vapor and liquid-vapor states. Here, the Homogeneous Equilibrium Model (HEM) is implemented to compute liquid-vapor properties. The internal energy and the density are considered as the two independent variables, which make a direct connection with any CFD solver based on this conservative formulation. Two validation cases, namely a shock tube and a converging-diverging nozzle, were performed to assess the performance of the tabulated EoS in terms of accuracy and efficiency. The proposed tabulated EoS exhibits an accuracy comparable to the original Span-Wagner EoS and a very significant gain in terms of computational time.

NOMENCLATURE

Acronyms

CFD	Computational Fluid Dynamics
COP	Coefficient of Performance EoS Equation of State
EoS	Equation of State
GWP	Global Warming Potential
HEM	Homogeneous Equilibrium Model
ODP	Ozone Depletion Potential

Symbols

A	Specific Helmholtz free energy	($J.m^3kg^{-1}$)
e	Specific internal energy	(Jm^3kg^{-1})
Ma	Mach number	(-)

p	Pressure	(Pa)
t	Time	(s)
T	Temperature	(K)
u	Velocity along x	($m.s^{-1}$)
v	Specific volume	(m^3kg^{-1})
x	Vapor quality	(-)

Greek letters

δ	Reduced density	(-)
γ	Interpolation coefficient for p	(-)
φ	Dimensionless Helmholtz free energy	(-)
ρ	Density	($kg.m^{-3}$)
τ	Reduced temperature	(-)

Subscripts

L	Left State
R	Right state
ref	Reference
δ	Derivative respect to the reduced density
τ	Derivative respect to the reduced temperature

Superscripts

r	Residual part of the dimensionless Helmholtz free energy
0	Ideal part of the dimensionless Helmholtz free energy
~	Properties in the transformed space

REFERENCES

Ameli, A., Afzalifar, A., & Turunen-Saaresti, T. (2017). Non-equilibrium condensation of supercritical carbon dioxide in a converging-diverging nozzle. *J. Phys.: Conf. Ser. 821*, 012-025.

Angielczyk, W., Bartosiewicz, Y., Butrymowicz, D., & Seynhaeve, J.-M. (2010). 1D modeling of supersonic carbon dioxide two-phase flow through ejector motive nozzle. *Proceedings of 13th International Refrigeration and Air Conditioning Conference at Purdue*, (2362), West Lafayette, USA.

Colarossi, M., Trask, N., Schmidt, D., & Bergander, M. (2012). Multidimensional modelling of condensing two-phase ejector flow. *Int. J. Refrig*, 35,290–299.

De Lorenzo, M., Lafon, P., DiMatteo, M., Pelanti, M., Seynhaeve, J. M., & Bartosiewicz, Y. (2017). Homogeneous two-phase flow models and accurate steam-water table look-up method for fast transient simulations. *Int. J. Multiphase Flow*, 95,199–219.

Elbel, S. & Hrnjak, P. (2006). Experimental validation and design study of a transcritical CO_2 prototype ejector system. *Proceedings of 7th IIR-Gustav Lorentzen Conference on Natural Working Fluids*, (28-31), Trondheim, Norway.

Elbel, S. & Hrnjak, P. (2008). Experimental validation of a prototype ejector designed to reduce throttling losses encountered in transcritical R744 system operation. *Int. J. Refrig*, 31,411–422.

Godunov, S. (1959). A difference method for numerical calculation of discontinuous solutions of the equations of hydrodynamics. *Mat. Sb.*, 47,271–306.

Khatami, F., Weide, E. V. D., & Hoeijmakers, H. (2015). Multiphase thermodynamic tables for efficient numerical simulation of cavitating flows: A novel look-up approach toward efficient and accurate tables. *Heat Transfer Eng.*, 36,1065–1083.

Kunick, M., Kretzschmar, H. J., & Gampe, U. (2008). Fast calculation of thermodynamic properties of water and steam in process modelling using spline interpolation. *Proceedings of International Conference on the Properties of Water and Steam*, (8-11), Berlin, Germany.

Lemmon, E. W., Huber, M. L., & McLinden, M. (2010). NIST standard reference database 23: reference fluid thermodynamic and transport properties. In *REFPROP*, Gaithersburg, USA. National Institute of Standards and Technology; Standard Reference Data Program.

LeVeque, R. J. (1997). Wave propagation algorithms for multi-dimensional hyperbolic systems. *J. Comput. Phys.*, 131, 327–353.

LeVeque, R. J. and Berger, M. J. (2017). Clawpack software. Version 4.3.

Li, D. & Groll, E. D. (2004). Transcritical co_2 refrigeration cycle with ejector-expansion device. *Proceedings of 10th International Refrigeration and Air Conditioning Conference at Purdue*, West Lafayette, USA.

Li, D. & Groll, E. D. (2005). Transcritical co_2 refrigeration cycle with ejector-expansion device. *Int. J. Refrig.*, 28,766–773.

Nakagawa, M., Berana, M. S., & Kishine, A. (2009). Supersonic two-phase flow of co_2 through converging-diverging nozzles for the ejector refrigeration cycles. *Int. J. Refrig.*, 32,1195–1202.

Palacz, M., Haida, M., Smolka, J., Nowak, A., Banasiak, K., & Hafner, A. (2016). HEM and HRM accuracy comparison for the simulation of co_2 expansion in two-phase ejectors for supermarket refrigeration systems. *Appl. Therm. Eng.*, 115,160–169.

Raman, S. K. & Kim, H. D. (2018). Solutions of supercritical co_2 flow through a converging-diverging nozzle with real gas effects. *Int. J. Heat Mass Transfer*, 116,127–135.

Smolka, J., Bulinski, Z., Fic, A., Nowak, A., & Banasiak, K. (2013). A computational model of transcritical R744 ejector based on a homogeneous real fluid approach. *Appl. Math. Model.*, 37, 1208–1224.

Span, R. & Wagner, W. (1994). A new equation of state for carbon dioxide covering the fluid region from the triple-point temperature to 1100 K at pressures up to 800 MPa. *J. Phys. Chem. Ref. Data*, 25(6):1509–1596.

Toro, E. F. (1997). *Riemann solvers and numerical methods for fluids dynamics*. Heidelberg, Germany, Springer-Verlag.

Toro, E. F., Spruce, M., & Speares, W. (1994). Restoration of the contact surface in the HLL Riemann solver. *Shock Waves*, 4, 25–34.

Yazdani, M., Abbas, A., & Radcliff, T. (2012). Numerical modelling of two-phase supersonic ejectors for work-recovery applications. *Int. J. Heat Mass Transfer*, 55, 5744–5753.

ACKNOWLEDGEMENT

Yu Fang and Sébastien Poncet acknowledge the support of the NSERC chair on industrial energy efficiency established in 2014 at Université de Sherbrooke funded by Hydro-Québec, Natural Resources Canada and Rio Tinto Alcan.